Biologic Origin of Iron Nodules in a Marine Terrace Chronosequence, Santa Cruz, California

Marjorie S. Schulz*
Davison Vivit
U.S. Geological Survey
345 Middlefield Rd. MS-420
Menlo Park, CA 94025

Charles Schulz
Knox College
Galesburg, IL 61401

John Fitzpatrick
Art White
U.S. Geological Survey
345 Middlefield Rd. MS-420
Menlo Park, CA 94025

The distribution, chemistry, and morphology of Fe nodules were studied in a marine terrace soil chronosequence northwest of Santa Cruz, California. The Fe nodules are found at depths <1 m on all terraces. The nodules consisted of soil mineral grains cemented by Fe oxides. The nodules varied in size from 0.5 to 25 mm in diameter. Nodules did not occur in the underlying regolith. The Fe-oxide mineralogy of the nodules was typically goethite; however, a subset of nodules consisted of maghemite. There was a slight transformation to hematite with time. The abundance of soil Fe nodules increased with terrace age on the five terraces studied (aged 65,000–226,000 yr). Scanning electron microscopy (SEM) revealed Fe-oxide-containing fungal hyphae throughout the nodules, including organic structures incorporating fine-grained Fe oxides. The fine-grained nature of the Fe oxides was substantiated by Mössbauer spectroscopy. Our microscopic observations led to the hypothesis that the nodules in the Santa Cruz terrace soils are precipitated by fungi, perhaps as a strategy to sequester primary mineral grains for nutrient extraction. The fungal structures are fixed by the seasonal wetting and dry cycles and rounded through bioturbation. The organic structures are compacted by the degradation of fungal C with time.

Abbreviations: ICP-MS, inductively couple plasma mass spectrometry; SEM, scanning electron microscopy; XRD, x-ray diffraction.

It is an understatement to say that studies of Fe in soils are abundant. The distribution of Fe in a soil is an important parameter of soil development. In addition, soil Fe oxides are a major contributor in adsorption and cation exchange reactions, and participate in oxidation–reduction reactions. Soil nodules and concretions of Fe and Mn are common and have been reported to occur worldwide. Recently, Fe soil nodules have been the subject of much work on the sequestration of heavy metals (Manceau et al., 2003; Cornu et al., 2005). As in many soils, the chronosequence soils in this study contain hard Fe nodules in the top 1 m.

The Santa Cruz soils are not unique; Fe-rich soil nodules occur in many soils of coastal California. Emery (1950) reported up to 50% (w/w) Fe nodules in the soil on the Loma Vista terrace in San Diego County (reported to be 1,000,000–1,200,000 yr). Nodules occur in soils of marine terraces on the offshore islands in southern California (Johnson, 1972, 1988; Muhs, 1982) and in coastal soils of Monterey and Santa Barbara counties (Don Johnson, personal communication, 2009). Moody and Graham (1995), in a study of marine terraces near Santa Barbara, reported up to 70% (w/w) nodules above a 1-m depth on their oldest terrace, which they dated as 560,000 yr. Nodules have also been found in marine terrace soils near Mendocino (personal observation, 2005). In a few of these studies, some nodules were recognized as being magnetic.

Studies of lateritic Fe pisolites are numerous and there is a temptation to compare these with temperate soil nodules. Tropical to subtropical lateritic soils, however, may not be good analogs for the temperate processes forming the nodules at the Santa Cruz sites. Nevertheless, some researchers have used the presence of

Soil Sci. Soc. Am. J. 74:550–564
Published online 19 Jan. 2010
doi:10.2136/sssaj2009.0144
Received 14 Apr. 2009.
*Corresponding author (mschulz@usgs.gov).

Fe–Mn nodules in a soil to indicate subtropical to tropical climates. A review of the literature reveals that temperate soils that have not been subjected to tropical weathering do contain nodules (Schwertmann and Fanning, 1976; Arocena and Pawluk, 1991; Brown and Thorp, 1942).

Detailed studies of the soil mineralogy, chemical weathering, hydrology, and weathering rates have been completed on the Santa Cruz terrace chronosequence (Munster and Harden, 2002; White et al., 2008, 2009; Maher et al., 2009). The current study builds on the previously published work at these sites. The goal of the current study was to understand the processes of nodule formation. To this end, we identified trends in nodule abundance with soil age and soil depth, and analyzed nodule chemistry, mineralogy, and morphology.

SITE DESCRIPTION

The coastal marine terraces west and north of Santa Cruz, CA (Fig. 1), consist of bedrock platforms covered by sediment. The bedrock platforms were planed into the Santa Cruz mudstone and Santa Margarita sandstone formations (both of Miocene age) by wave action during periods of high sea level. The combined effects of tectonic uplift and periodic changes in sea level created emergent wave-cut platforms that are blanketed with 1 to 10 m of sediment (Bradley and Griggs, 1976). The terrace sediments are derived principally from the granitic core of the Santa Cruz Mountains, but also include material from local sedimentary formations. The terrace deposits, which blanket the wave-cut platform, have been characterized as reworked beach and shallow marine deposits left by a regressing sea (Bradley, 1957), and as near-shore marine sediments overlain by fluvial, colluvial, and aeolian deposits (Weber and Allwardt, 2001). The presence of clays in the terrace sediments, first noted by Bradley (1957) and identified by White et al. (2008) as a Fe-rich smectite, further constrains the depositional environment to shallow marine. Marine terrace formation as modeled by Trenhaile (2005) showed that the fine-grained (smectite clay) shallow marine facies can be secluded and preserved from wave base erosion by the armoring effect of drifting coarse-grained beach sediments during a sea-level regression or transgression.

The soil formation on the terrace deposits began as they emerged during sea-level regression and continues to the present. The highest terraces have the oldest and most highly weathered soils. The soil series and soil classifications for our sites are found in Table 1. The sampling sites are all located on Mollisols. The soils are currently occupied by a coastal prairie ecosystem with predominately non-native European annual grasses. We've

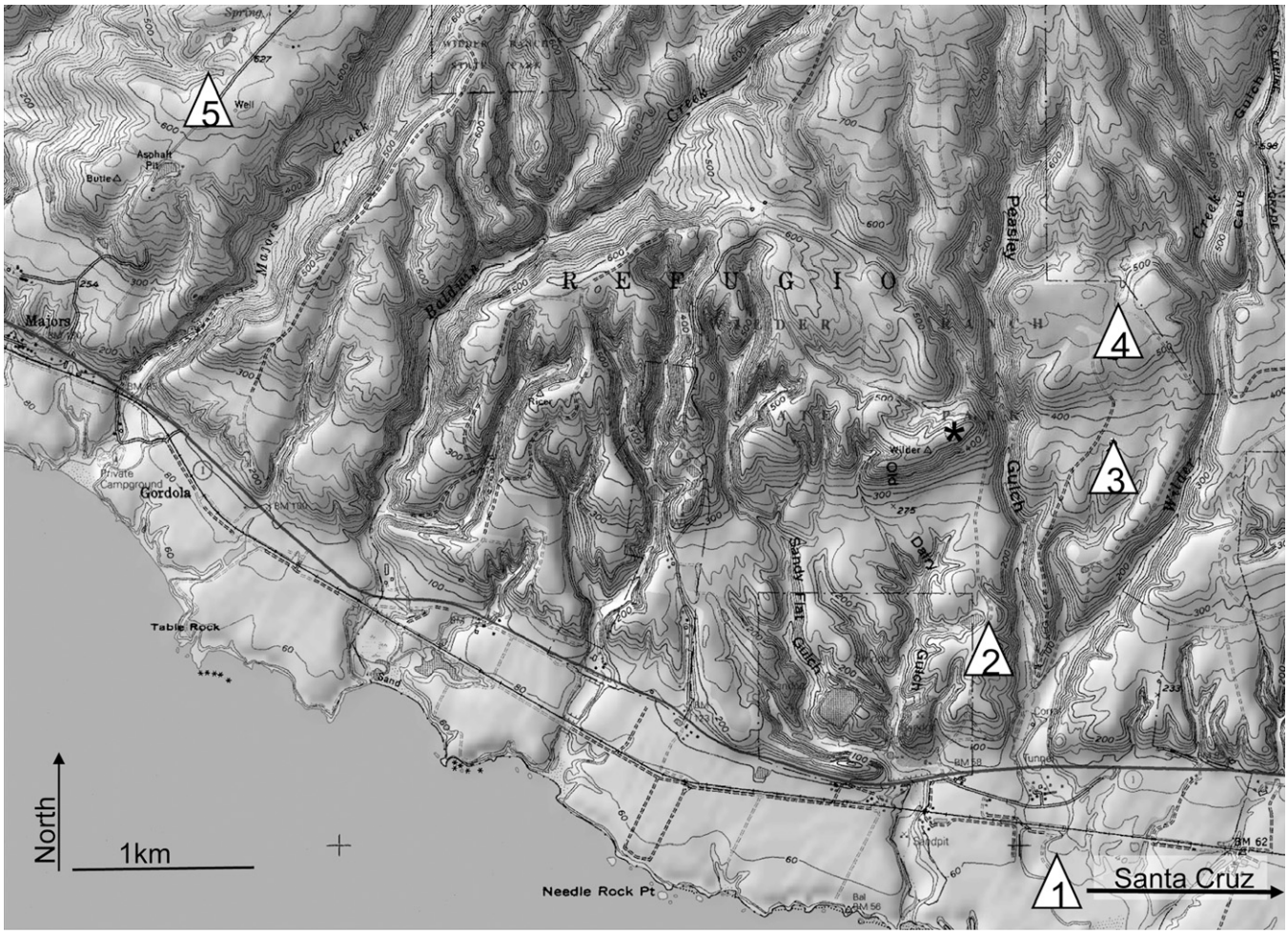

Fig. 1. Map and location of sampling sites. The SCT1 site is located approximately 5 km east of map area. Instrumented sites are indicated with triangles, duplicate soil sample from SCT4 indicated with a star.

Table 1. Soils formed on the marine terraces north of Santa Cruz.

Terrace designation	Soil series†	Taxonomic classification	
		Soil survey†	Aniku and Singer (1990)
Terrace 1, SCT1	Pinto loam	fine-loamy, mixed, thermic Typic Argixeroll	coarse-loamy, mixed, mesic Typic Argixeroll
Terrace 2, SCT2	Pinto loam	fine-loamy, mixed, thermic Typic Argixeroll	
Terrace 3, SCT3	Pinto loam	fine-loamy, mixed, thermic Typic Argixeroll	fine-loamy, mixed, mesic Ultic Argixeroll
Terrace 4, SCT4	Los Osos loam	fine, montmorillonitic, thermic Typic Argixeroll	fine-loamy, mixed, mesic Ultic Haploxeralf
Terrace 5, SCT5	Watsonville loam	fine, montmorillonitic, thermic Xeric Argiaboll	clayey, mixed, mesic Typic Haploxerult

† According to the soil survey of Santa Cruz County, California (Bowman and Estrada, 1980).

included the soil classifications from Aniku and Singer (1990) for comparison. Their study occurred on sites closer to the city of Santa Cruz. Detailed soil descriptions and analyses from our sites can be found in Munster and Harden (2002) and from the Aniku and Singer sites in Pinney et al. (2002).

The uplifted marine terraces provide a natural laboratory to study pedologic, geologic, and geochemical processes with time. We took advantage of the fact that the older surfaces are preserved through tectonic uplift and used them to study pedogenic processes through time. The age dates used are from Perg et al. (2001). This central California site currently has a Mediterranean climate (cool wet winters, warm dry summers). The summer temperatures are moderated by fog. The terraces studied are under the orographic rainfall influence of Ben Lomand Mountain; the higher terraces receive more rainfall than the lower (White et al., 2009). The average annual rainfall for the city of Santa Cruz, CA, is 727.2 mm (28.5 inches); the average temperature is 13.4°C (56°F).

MATERIALS AND METHODS

Initial surveys, conducted by hand auguring and field observations, indicated significant variations in depth and relative coarseness of the terrace deposits. Five sites, one on each terrace, were selected from this survey for intensive characterization. The selection criteria included: a lack of significant physical erosion based on the lateral persistence of level topographical surfaces, a sufficient lateral distance from the toe and edges of paleo sea cliffs, and the apparent lack of anthropogenic influences, particularly agriculture on the younger terraces. Unfortunately, anthropogenic disturbance of the SCT4 surface was detected after it was fully instrumented. The selected sites also have deep terrace sediments (4–15 m), which provide sampling environments that extend below the zone of significant biological mixing.

Soil nodule abundances were determined in air-dried soil samples from 10-cm depth intervals on each terrace to the 100-cm depth. Soil sample weights for nodule abundance determination were 500 to 1000 g. Size separations of nodules were done by wet sieving to the following size fractions: >5.6, 5.6 to 4, 4 to 2, 2 to 1, and 1 to 0.5 mm. In all size fractions >2 mm, magnetic nodules were removed with a hand magnet and nonmagnetic nodules were hand separated from any sediment present. These subsamples were weighed. Although nodules occurred in the <2-mm size fraction, the focus of this study was on nodules >2 mm in size.

A representative subsample of nodules from each terrace soil was taken from the 20- to 30-cm soil depth interval, using the 2- to 4-mm size fraction, and ground to a powder. Nodule chemistry (by inductively coupled plasma mass spectrometry [ICP-MS]), x-ray diffraction, Mössbauer spectroscopy, and total C content were performed on subsamples of the ground mixture of nodules. Chemistry was done with a PerkinElmer ICP-MS (PerkinElmer Corp., Waltham, MA) using total dissolution by HF and HNO_3. Total C and total N were determined by combustion at 1020°C on a Carlo Erba NA1500 elemental analyzer (Carlo Erba, Milan). It should be noted that, if present, CO_3–C would be part of the total C; however, these soils are acidic, so no CO_3–C was expected and none has been detected. The C and N concentrations of all soil samples were compared with a main working standard as delineated in Manies et al. (2006). Digital field-emission scanning electron microscopy (SEM) was done on a Leo 982 (Carl Zeiss SMT, Peabody, MA). Samples were prepared for the SEM by vacuum coating with Au.

Mössbauer spectra were collected using a Ranger Scientific MS-900 spectrometer, with a VT-900 transducer in constant acceleration mode (Ranger Scientific, Burleson, TX). Spectra were transferred to a PC and stored for later analysis. The Mössbauer source from Ritverc had an initial activity of 3,7 GBq of ^{57}Co embedded in a rhodium foil. Gamma ray counts were detected by a Reuter-Stokes Kr-CO_2 proportional counter (GE Reuter-Stokes, Twinsburg, OH). The samples were cooled in a CRYO Industries of America (Manchester, NH) closed-cycle cryostat, and sample temperature was controlled to ±0.1°C by a Lake Shore Cryotronics 805 controller (Lake Shore Cryotronics, Westerville, OH). Mössbauer samples were packed into thin-walled Delrin sample cups, and all spectra were taken in an applied field of 0.05 T perpendicular to the γ-ray beam.

RESULTS

Iron Nodule Morphology

Macroscopic Morphology

Macroscopically, the unbroken nodules looked reddish brown to dark red. They were usually coated with soil matrix and were difficult to visually pick out of freshly sampled soil. They were hard, however, could not be hand crushed, and were easily found by feel. They were generally spherical or oblate spheroids. Approximately 20% were oddly shaped, with bulges and elongate extensions. The odd-shaped nodules tended to be in the large size fractions (>4 mm). Few of the magnetic nodules were irregularly formed; most were oblate spheroids. The outside of a nodule often had protruding mineral grains (most often quartz). In the dark red nodules, the outer surface could have a shiny appearance when the soil matrix was washed off. This gave the look of dissolution having occurred on the exterior of the nodule.

More than 100 nodules (>2 mm) were cut or broken open to examine morphologic diversity. The nodules were surprisingly porous for their strength. In cross-section, nodules >4 mm in

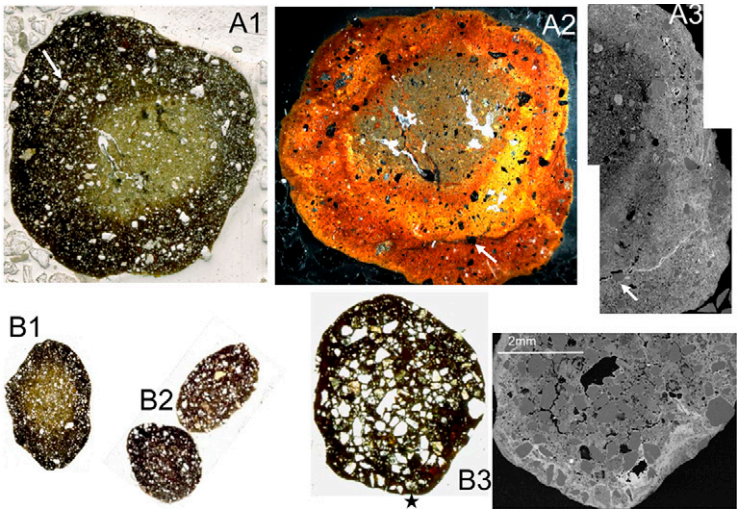

Fig. 2. Micromorphology of Fe nodules: (A1) a 1-cm-diameter nodule from SCT5 taken with transmitted light; (A2) the same nodule with reflected light; (A3) a composite of two scanning electron microscope (SEM) backscatter images of the same nodule, where Fe-rich areas are brighter (in these images, the white arrows point to the same mineral grain; note the correlation between the darkest zone in A2 and the Fe-rich zone in A3); (B1) a nodule from SCT3 that is characteristic of the large nodules having a dense Fe-cemented outer rind with a less cemented center (the long dimension of the nodule is 1.1 cm); (B2) the characteristic morphology of smaller nodules, with dense Fe cement through the entire nodule, both from SCT3 and 0.6 cm in the long dimension; (B3) two images of a nodule from SCT5 (long dimension is 0.6 cm) where dark zones on the lower right of the transmitted light image correspond to the brightest area of the SEM backscatter image. Energy dispersive spectroscopy revealed the bright areas to be Fe oxides. The feldspar grain above the star is extensively tunneled with Fe-rich hyphae, creating a smoky look in the transmitted light image.

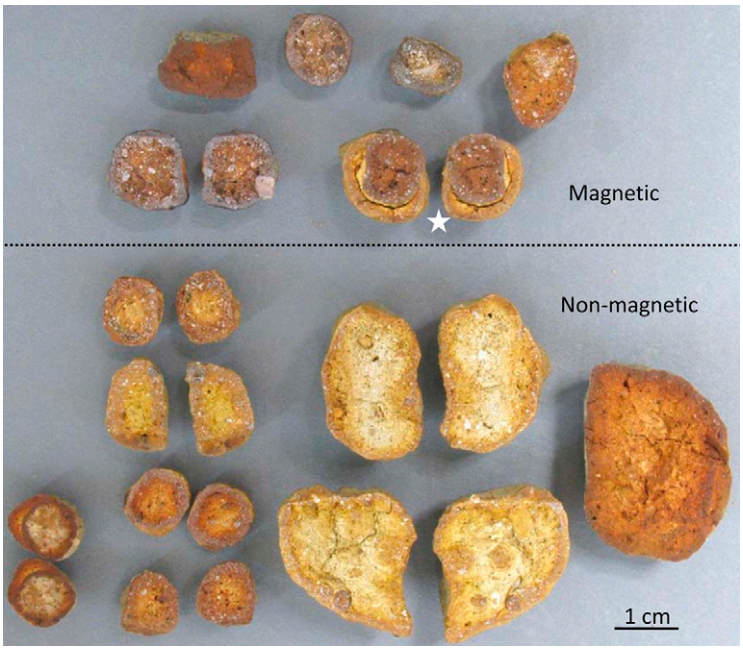

Fig. 3. Assorted opened nodules from SCT3 at various soil depths to illustrate internal morphology. Note how all nodules have a rind that is harder than the center. The internal morphology of nonmagnetic nodules are heterogeneous, showing compound morphology with inclusions of smaller nodules, double rinds, nodules with friable centers, and massive nodules. Smaller nodules tend to have a macroscopically undifferentiated or massive internal structure. The magnetic nodules have a darker brick-red color and generally have massive internal morphology. The starred sample has a partial double rind; note the sediment caught between the inner and outer rinds.

diameter consisted of Fe oxides cementing sediment with a hard outer rind. The nodules <4 mm in size were mostly internally homogeneous. The interior color of a nodule ranged from dark reddish brown (2.5YR 3/3) to very pale brown (10YR 7/4). The magnetic nodules tended to be dark reddish brown (2.5YR 3/4) throughout. The large nonmagnetic nodules (>4 mm) most often had a dark reddish brown (2.5YR 3/4) to reddish brown (5YR 5/4) outer rind with a very pale brown center (10YR 7/4) (Fig. 2). The diversity of internal structures was higher in the large nodules than the smaller nodules. Some of the larger nodules contained what looked to be entrained smaller nodules (Fig. 3). A few nodules were obviously broken in the soil. None of the nodules at Santa Cruz exhibited concentric layers, as reported for nodules in some areas (Phillippe et al., 1971; Singh and Gilkes, 1996; Palumbo et al., 2001; Latrille et al., 2001; Stiles et al., 2001; Liu et al., 2002)

Microscopic Morphology

Microscopically, the nodules were complex structures of primary mineral grains cemented by Fe oxides, clay minerals, and fungal hyphae. In thin section with transmitted light, the Fe in the nodules was generally opaque; however, occasionally there were transparent-red to brick-red microcrystalline areas showing wavy extinction with a petrographic microscope. The ochre-yellow centers of larger nodules were generally transparent in transmitted light, and the Fe oxides appeared uniformly distributed. Under incident or reflected light, the complexity of the nodule became apparent (Fig. 2). The Fe-rich areas of a nodule wandered among less densely cemented Fe oxides and soil sediments (Fig. 2).

All nodules examined by SEM contained fungal hyphae. In addition, the nodules all had areas of high Fe content that were usually associated with spherical vesicles approximately 5 μm in diameter (Fig. 4). Thin-sectioned nodules, imaged with SEM in backscattered mode, highlighted areas high in Fe content, which were the brightest zones within the nodules (Fig. 5). Energy dispersive spectroscopy analyses (not shown) of these zones revealed a simple chemistry of Fe, O, and C. After examining many nodules, it became apparent that the high-Fe zones had a similar morphology in all the nodules; however, the particular morphologic features present in any one thin-sectioned nodule were dependent on the geometry of the thin section plane relative to the high-Fe zone. In cross-section parallel to the Fe trend, the areas of high Fe were elongated, with a narrow seam of spherical vesicular features in the core (Fig. 5). In a thin section perpendicular to the trend of high Fe, the area was oblate to amoeboid in shape, with centrally located vesicles (Fig. 6). The vesicles were usually lined with fungal hyphae, which also contained or were encrusted with Fe oxides (Fig. 4). Many thin-sectioned nodules also included an oval structure

(up to 1 mm in diameter) made up of circular "cells;" these "cells" were filled with small vesicles (Fig. 7).

Fungal tunneling into primary mineral grains within the nodules was common, especially in the nodules of the older terraces. Fungal hyphae occupying tunnels within mineral grains also contained Fe and appeared in an optical microscope as dark lines penetrating the grain. This observation supports a hypothesis that the Fe is actively precipitated within fungi, because diffusion and precipitation of Fe into small tunnels or cracks in a feldspar grain (which has no Fe in the primary crystal structure) would be a slow and less pervasive process. Within the nodules, areas of high Fe often wrapped around or encapsulated mineral grains (Fig. 5). Mineral grains surrounded by areas of high Fe appeared often enough in the nodules to create the idea that there may be purpose to it.

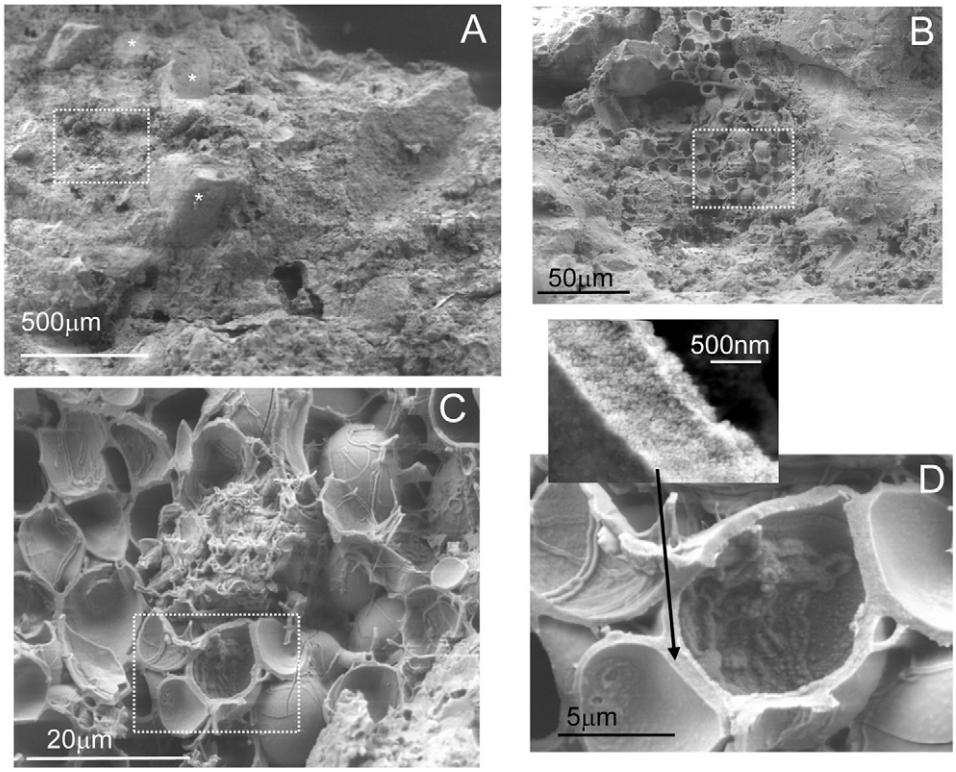

Fig. 4. Scanning electron micrographs of a nodule from SCT2, 25-cm soil depth taken at low voltage (5 kV) and of the same area with increasing magnification: (A) a large portion of the broken open nodule with primary mineral grains cemented in the Fe matrix marked with a star; (B) enlargement of the indicated area in A showing the vesicular structure tentatively correlated to microcolonial fungi; (C) enlargement of B—the vesicular structures are always associated with fungal hyphae; (D) enlargement of the indicated area in C, with hyphae visible inside the vesicles. The inset to D is an enlargement of the vesicle wall; at this magnification Fe is seen as small particles within the structure.

Mineral grains within the nodules showed features of mineral dissolution, expressed as cavities between the mineral grain and the Fe-oxide matrix. In some cases, replacement of mineral grains by Fe oxides had occurred. Inside a few of the nodules, we found that Fe replaced plant-derived material.

Iron Nodule Abundance

Nodules were found from the soil surface to a depth of 1 m (Table 2), with average concentrations generally increasing with soil age (SCT1 = 1.23, SCT2 = 1.22, SCT3 = 1.55, SCT4 = 1.44, and SCT5 = 3.28% w/w). In the younger terrace soils (SCT1 and 2), nodule abundances were relatively consistent with depth. In SCT3 and SCT5, nodules were most abundant above 50 cm, with the abundance dropping to near zero below this depth (Fig. 8). To examine heterogeneity in nodule abundance, duplicate profiles were sampled from several terraces (Fig. 8). Profile SCT1 showed significant variability with depth. The SCT1A site, however, had consistent nodule abundance with depth. These samples were taken within 100 m of one another. On SCT2, abundance profiles were surprisingly similar and also sampled within 100 m of each other. The SCT5 profiles were also sampled within 100 m of each other and showed the highest variability in abundance. There were no trends in nodule size with soil age (Fig. 9).

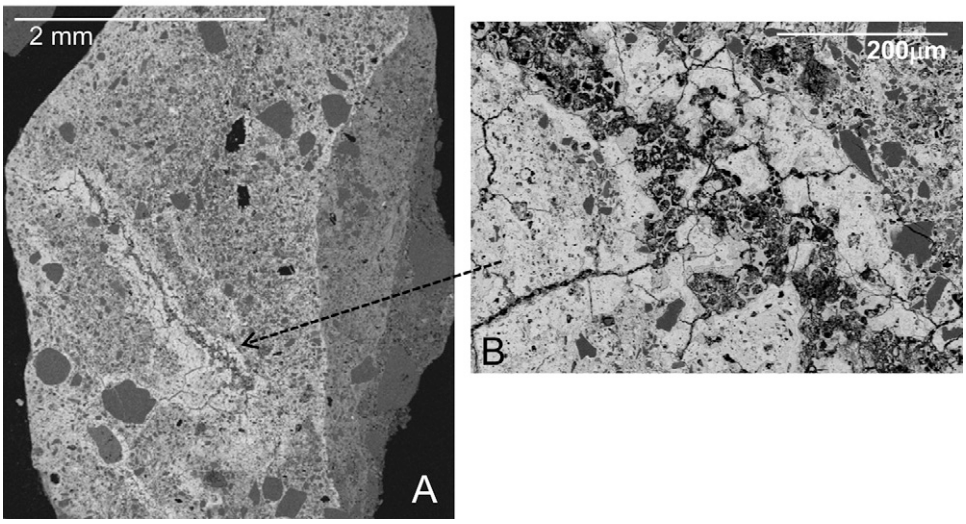

Fig. 5. A thin-sectioned nodule from SCT5: (A) scanning electron microscope backscatter image showing an area of high Fe (white) with a central vesicular zone oriented diagonally across the nodule, and mineral grains (gray) surrounded by areas of high Fe in the lower half of the nodule; and (B) an enlargement of the high-Fe area crossing the nodule in A.

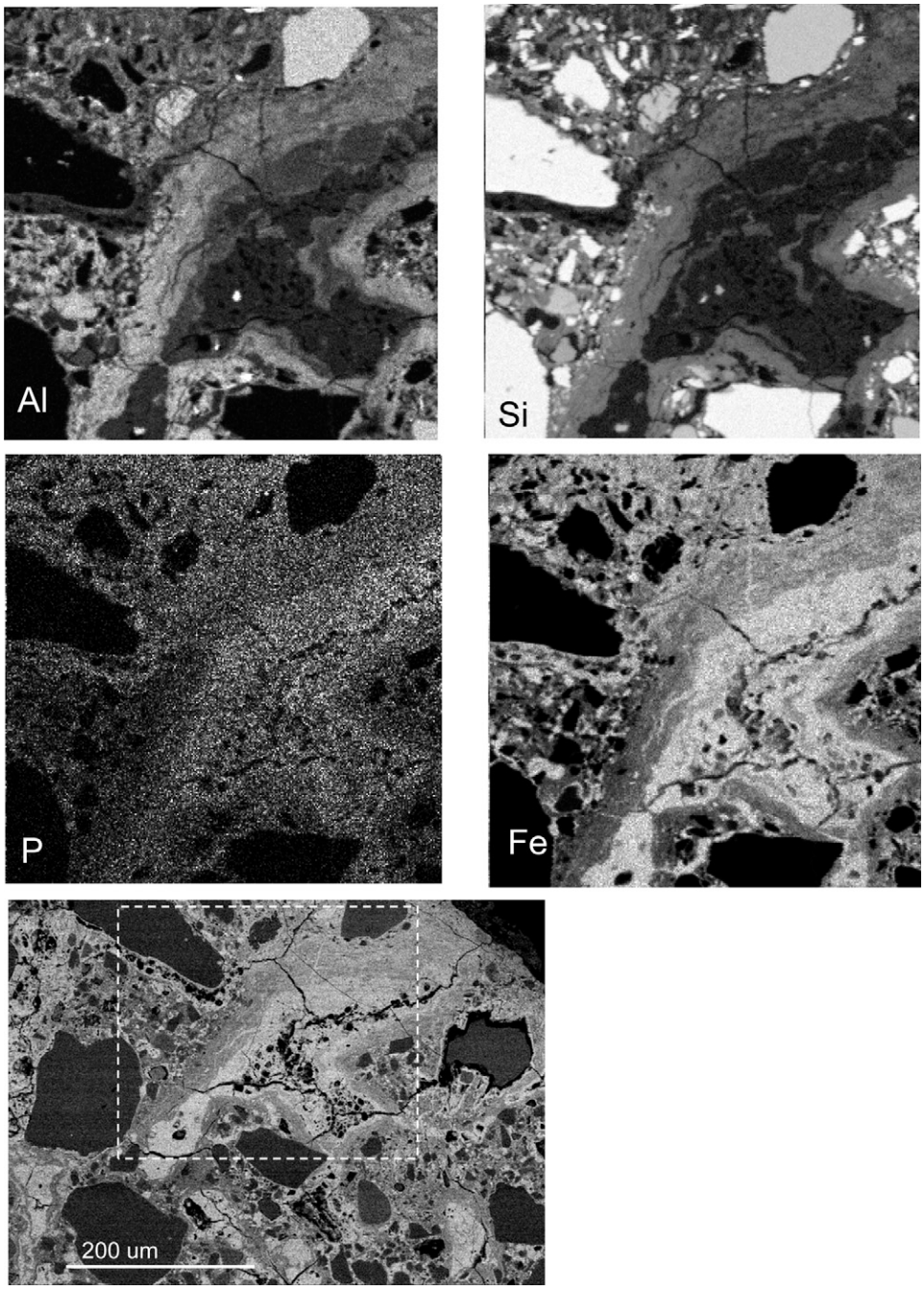

Fig. 6. Elemental maps done with an electron microprobe of an SCT2 nonmagnetic nodule and a scanning electron microscope backscatter image of the same area. Note the amoeboid shape of the main high-Fe area and the vesicles at its center. Iron is the only constituent in the brightest backscatter zone. Phosphorus, although not abundant, is correlated with the Fe.

Two SCT4 profiles were sampled from sites on either side of Peasley Gulch (a 700-m-deep stream valley), approximately 1 km apart. Due to anthropogenic alteration, the instrumented SCT4i site (Fig. 8, open squares) deviated from the trend of increasing nodule abundance with increasing soil age. It appeared that up to 30 cm of the A horizon had been removed at this site. The nodule distribution was truncated by the disturbance. A second SCT4 nodule profile was collected on the nearby ridge (Fig. 8, filled squares). The second profile, SCT4r, contained nodules to a 1-m depth; however, the average abundance of the nodules was still lower than SCT3. The SCT4r sample site is a small erosional remnant (Fig. 1), located within 4 m of the paleo sea cliff. The nodule abundance there was probably impacted by erosion and hydrologic processes. The proximity to the paleo sea cliff affected the hydrology of this site; water drains faster. The nodule abundance on this small terrace remnant suggests that soil moisture may be a factor in nodule accumulation and preservation.

Iron Nodule Chemistry

Nodule chemistry, as analyzed by ICP-MS, is presented in Table 3. The analyses revealed that magnetic nodules had a higher Fe_2O_3 concentration (37–42% w/w) than the nonmagnetic nodules (23–31% w/w). In general, the Fe_2O_3 content of the nodules increased with the age of the terrace (Fig. 10). The SCT3 nodules are the exception and had lower Fe_2O_3 contents than the SCT2 nodules. In contrast, the average Fe_2O_3 content of the bulk soils (in the <2-mm size fraction, above 2-m soil depth) ranged from 3.0 to 4.6% (w/w). Adding the nodule Fe_2O_3 content to the bulk soil concentration raises Fe_2O_3 bulk soil averages to 3.2 to 6.25% (w/w). Removing large Fe or Mn nodules by removing the >2-mm size fraction before a bulk chemical analysis can cause low totals of these elements in nodule-containing soils.

The nodules of the Santa Cruz terrace soils had a low Mn content. The amount of MnO in the nodules decreased with terrace age, from 2350 mg kg^{-1} in SCT1 (nonmagnetic nodules) to 280 mg kg^{-1} in SCT5 (Table 3). The MnO in the magnetic nodules decreased from 780 to 260 mg kg^{-1} with terrace age. Manganese was concentrated in the nodules rather than the bulk soils. Soil MnO levels fell from 500 mg kg^{-1} in SCT1 to 200 mg kg^{-1} in SCT5. In contrast to the nodules in these soils, soil nodules from other sites had Mn contents higher than Fe (Uzochukwu and Dixon, 1986). Manganese concentrations in nodules have been correlated to nodule size and soil depth (Phillippe et al., 1971; Zhang and Karathanasis, 1997), as well as precipitation amount (Stiles et al., 2001). Although Mn

levels in nodules are somewhat determined by the amount of Mn in the parent material, in some areas it may also be a clue to the process of nodule formation. The formation of the nodules in the Santa Cruz terrace soils concentrated Mn, yet with time the Mn content of the nodules dropped to near soil levels, indicating a flux of Mn from the nodules and the soil with time.

Phosphorus was concentrated in the nodules relative to the P in the bulk soil (White et al., 2009; Fig. 10). In contrast, the Ca concentration was higher in the bulk soils than in the nodules for the younger terraces but decreased to comparable concentrations for the older terraces. The bulk soil Ca concentration reflects the extensive loss of Ca during hornblende and plagioclase weathering in the bulk soil. Both Ca and P are readily sorbed by Fe oxides, and as nutrients, the preservation of relatively high concentrations of these leachable components makes the nodules potential targets for concentrated biologic activity. Indeed, there has been much work on the sorption of P and Ca by Fe oxides. It has been shown that P was sorbed and held tightly by Fe-rich soil nodules (Tiessen et al., 1993). It is curious then that the P_2O_5 concentration in the Santa Cruz nodules decreased with time (Fig. 10). The loss of P with time seems to indicate that it is not irreversibly absorbed to the Fe oxides in the nodules and is therefore biologically available.

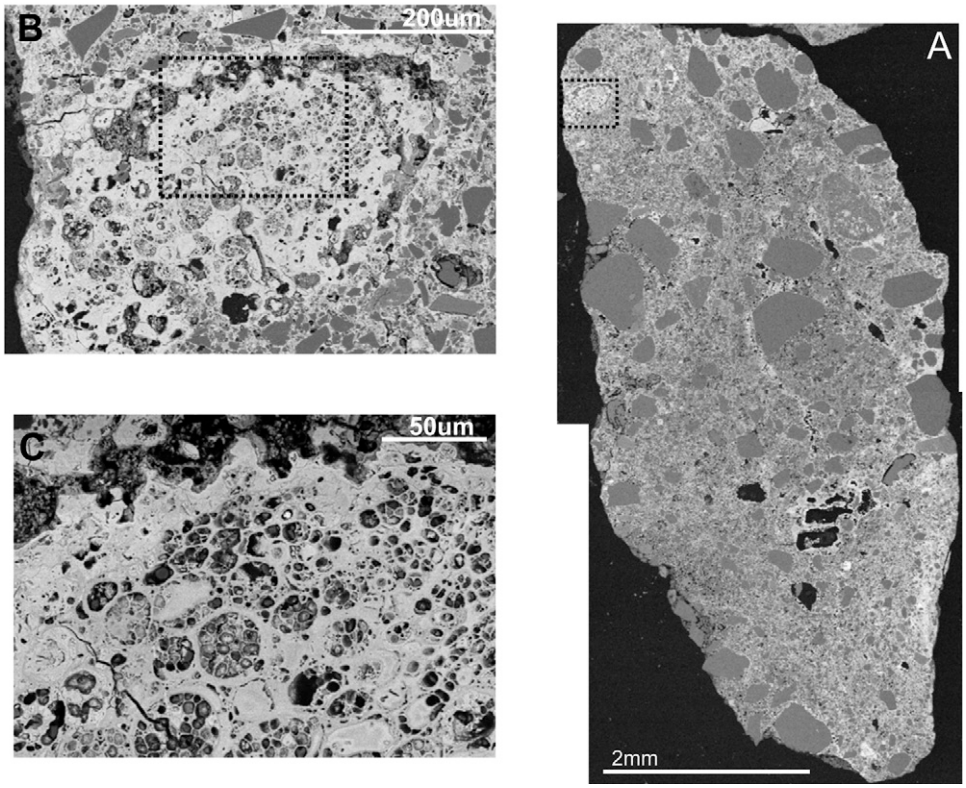

Fig. 7. Scanning electron microscope backscatter images of an SCT5 nodule with an oval structure (indicated by square on the top left). These structures were found in many nodules studied, although not always in such a regular oval shape: (A) a composite of two images to illustrate the whole nodule, with primary mineral grains evident as rounded gray areas; (B) close-up of the oval structure indicated in A; (C) close-up of B, showing the large "cell" morphology with small vesicles inside. These structures are mostly Fe with associated C containing trace Si and Al.

The total C concentration in the nodules is reported in Table 3 and Fig. 10. The C content of the nodules (0.57–0.99% w/w) was less than that of the shallow bulk soil (0–39 cm) and similar to the soil at the 40- to 100-cm depth, where C was consistently <1% (w/w).

Iron Nodule Microprobe Analyses

Electron microprobe elemental maps (Fig. 6) reveal the areas of highest Fe concentration and the complex relationship between it and other mineral phases. The lighter shades indicate higher concentrations of the mapped element; black indicates no detection of the element. The maps are qualitative, and actual elemental concentrations cannot be assigned. In the Al and Si panels, the quartz grains can be quickly differentiated from the feldspars through the lack of Al in the quartz. The high-Fe area is clearly delineated by the Fe map. Although P was present in low concentrations, the map of P shows that it is associated with the high-Fe area. These maps reveal undulating areas of Al and Si within the outer edges of the high-Fe area. The quartz grain in the upper left of the map is surrounded by the vesicular high-Fe structure often seen around mineral grains in the nodules.

Iron Nodule Mineralogy

X-ray diffraction (XRD) mineralogy analysis was done on a subsample of the ground nodule samples prepared for chemical analysis. The Fe phase in the nonmagnetic nodules was goethite, and in magnetic nodules was maghemite. In the nonmagnetic nodules, there was an increase in height and decrease in peak width at half peak height of the 0.269-nm peak from SCT1 to SCT5; this peak occurs in both goethite (hkl 130, intensity 35) and hematite (hkl 104, intensity 100) XRD patterns. No other goethite peaks showed a systematic increase in crystallinity. This seems to indicate a slight transformation to hematite with time rather than an increase in goethite crystallinity.

Iron Nodule Mössbauer Spectroscopy

Mössbauer spectroscopy provides information on Fe in mineral phases such as the oxidation state and coordination environment of Fe. In soils, Mössbauer spectroscopy has been used in the identification of Fe oxides, to understand the valance state of the Fe in minerals, to obtain information on particle size, and to study the magnetic state of Fe minerals. In these soils, there was no systematic change in the Mössbauer spectra of nodules with

Table 2. Nodule abundance in depth increments of bulk soil samples.

Terrace	Bottom depth of sampling increment	Total weight of nodules >2 mm	Proportion of nodules >2 mm	Total weight of magnetic nodules	Proportion of magnetic nodules
	cm	g	% w/w	g	% of total nodules
SCT1	8	13.0	2.5	0.7	5.1
	13	9.0	1.7	1.2	13.7
	18	15.0	2.9	0.1	0.8
	30	10.5	0.7	0.0	0.0
	38	17.7	2.2	0.0	0.0
	51	17.4	1.3	0.0	0.0
	61	44.6	3.0	0.7	1.6
	74	6.0	0.5	0.0	0.3
	84	0.8	0.1	0.0	0.0
	91	0.4	0.0	0.0	0.0
	100	0.0	0.0	0.0	0.0
SCT1A	15	7.0	0.4	0.0	0.0
	25	10.3	0.8	0.0	0.0
	40	28.9	1.9	0.0	0.0
	50	24.6	1.8	0.0	0.0
	65	25.3	2.1	0.0	0.0
	80	13.3	1.3	0.0	0.0
	90	3.0	0.3	0.0	0.0
	105	1.6	0.2	0.0	0.0
SCT2	10	3.3	0.9	1.5	45.9
	20	19.5	1.6	7.1	36.2
	25	7.8	1.2	4.2	54.4
	30	8.2	1.2	3.8	45.6
	40	9.6	1.2	4.6	48.2
	46	11.1	1.3	7.9	71.1
	56	10.5	1.5	4.1	38.9
	70	22.3	1.4	8.7	39.0
	80	8.9	0.6	3.6	40.7
SCT2a	13	9.9	1.4	2.9	29.1
	25	15.1	1.4	5.5	36.2
	38	10.0	1.3	5.8	57.6
	51	9.7	1.1	3.9	39.9
	58	11.7	1.4	5.3	45.4
	74	15.1	1.2	7.6	50.3
	84	6.6	1.1	1.8	27.0
	97	7.5	0.9	3.4	45.5
SCT3	10	31.6	3.8	9.9	31.5
	20	38.8	3.5	7.8	20.1
	30	43.2	3.3	10.9	25.1
	40	45.5	3.3	11.5	25.3
	50	25.6	1.3	6.1	23.9
	60	1.4	0.1	0.3	22.8
	70	2.0	0.1	0.5	24.1
	80	0.2	0.0	0.1	33.7
	90	0.0	0.0	0.0	0.0
	100	0.3	0.0	0.1	37.6
SCT4i	10	19.9	2.1	1.0	47.3
	20	10.1	0.7	0.5	67.3
	30	8.5	0.6	0.4	65.2
	40	2.1	0.2	0.0	15.5
	50	0.0	0.0	0.0	100.0
	60	0.7	0.0	0.0	100.0
SCT4r	15	35.0	2.4	9.6	27.4
	30	33.8	1.4	14.3	42.3
	43	40.5	1.8	16.6	41.1
	53	39.2	2.0	15.4	39.4
	66	38.1	1.8	12.2	31.9
	76	20.8	1.1	10.3	49.5
	84	10.1	0.6	5.1	50.8
	94	4.7	0.3	1.5	31.9

Continued next page.

soil age. The Mössbauer spectroscopy of nodule samples showed an isomer shift (δ) that ranged from 0.34 to 0.48 mm s^{-1}, indicative of fully oxidized Fe in the samples. Room-temperature Mössbauer spectra of the nonmagnetic (goethite) samples exhibited doublets. These same samples, when brought down to 15 K, exhibited magnetic ordering (Fig. 11). The magnetic ordering was manifest in the Mössbauer spectra through the appearance of a sextet spectrum below a characteristic temperature at which magnetic ordering becomes prevalent. The change in spectra with temperature is not uncommon in soils; it can be due to small crystallite size, water content, or Al substitution for Fe (Mitra, 1992; da Costa et al., 1995; Betancur et al., 2004). Although the water and Al contents of the Fe oxides were unknown, the temperature effect on the Mössbauer spectra of the nonmagnetic nodules could simply be due to the small crystallite size (as imaged by SEM; Fig. 4). The magnetic (maghemite) nodules had a Mössbauer spectrum (not shown) that was magnetically ordered at room temperature (similar to the nonmagnetic nodules at the lowest temperature in Fig. 11).

DISCUSSION

Background: Nodule Formation

The morphology of soil nodules is generally overlooked as an attribute important to understanding the nodule formation process. Nodules (concretions) with thin concentric layers to the nodule center (like an onion) are not generally found in the same soil as nodules without this layering, an exception being found by Kemp et al. (1998). Images of layered nodules can be found in Stiles et al. (2001) and in Singh and Gilkes (1996). None of the nodules in the Santa Cruz terraces exhibited concentric morphology. A majority of the Santa Cruz nodules had a cemented matrix; however, most of the

larger (>4-mm) nodules examined did exhibit a gross internal morphology of a friable inner core and a hard outer rind (Fig. 2 and 3). These were similar to the nodules described by Cornu et al. (2005).

An effort to include soil nodule morphology in soil nodule studies would allow the consideration of processes of formation and make comparisons between sites possible. For example, Fe/Mn ratios in nodules (<2 mm) was used to characterize paleoprecipitation during nodule formation by Stiles et al. (2001). They concluded that higher total Fe contents in soil nodules correlated with higher precipitation during formation. In the Santa Cruz terraces, we found the highest Fe concentrations in nodules on the oldest terrace, seemingly an effect of aging. There is also an orographic effect, however, of more precipitation on the older (higher) terraces at our sites (White et al., 2009). There is a temptation to apply the conclusions of Stiles et al. (2001) to our sites; however, the nodules described by Stiles et al. (2001) had concentric morphology, were formed under a different climate, had higher Mn content, and probably formed from different processes than the cemented-matrix Santa Cruz nodules.

Table 2 (continued).

Terrace	Bottom depth of sampling increment	Total weight of nodules >2 mm	Proportion of nodules >2 mm	Total weight of magnetic nodules	Proportion of magnetic nodules
	cm	g	% w/w	g	% of total nodules
SCT5	8	13.3	4.3	1.9	14.5
	13	37.8	7.7	8.3	22.1
	23	41.0	6.1	10.0	24.4
	36	48.4	6.8	12.2	25.2
	43	30.7	4.3	5.0	16.4
	51	6.3	0.8	0.9	13.6
	56	9.1	1.2	3.4	36.6
	64	39.5	6.5	6.8	17.2
	74	20.9	3.4	4.0	18.9
	83	0.5	0.1	0.1	25.0
SCT5a	10	16.8	4.0	4.3	25.9
	20	23.4	4.4	7.7	32.9
	30	22.3	3.3	5.9	26.7
	40	28.2	3.8	4.0	14.3
	50	9.2	1.2	2.2	24.2
	60	8.8	1.1	3.1	34.8
	70	13.6	1.3	4.2	30.7
	80	2.5	0.4	0.6	24.0

Morphologic subdivisions similar to those used here were also presented by Kovda et al. (1998); they described concentric (lit-par-lit) nodules and cemented matrix nodules as forming from different processes. Several studies have found soil nodules with concentric layering and cemented matrix nodules in soils occupying different landscape positions in the same study area (Phillippe et al., 1971; Singh and Gilkes, 1996; Palumbo et al., 2001; Gaiffe and Kubler, 1992). As the scientific community begins to interpret soil nodule occurrence and chemistry as environmentally determinant, the internal nodule morphology data are necessary to make comparisons between sites.

It seems probable that the processes that form cemented-matrix nodules in soils are different from those that form concentric nodules. In addition, there may be several ways of forming nodules of similar morphology. Cemented-matrix nodules, like those found in the Santa Cruz terrace soils, have been reported from many sites and not all have similar processes of formation. Johnson (1972) and Lindbo et al. (2000) have both proposed the formation of cemented-matrix nodules from the disintegration of dense material in the B horizon. In the study of Lindbo et al. (2000), Fe nodules in loessial soils of the lower Mississippi River Valley were shown to be a product of the degradation of a fragipan horizon and not specifically due to redox fluctuations. Nodules found on San Miguel Island, California, have also been interpreted to have formed from the disaggregation of the dense B horizon (Johnson, 1972). In that study, Johnson (1972) showed that nodules formed from weathering chloritic clay masses derived from the argillic horizon. In their study of Fe–Mn concretions from Bavaria, Germany, Schwertmann and Fanning (1976) studied concretions of a cemented-matrix morphology and concluded that wetting–drying cycles are important in nodule formation.

Some researchers have suggested that a biologic component may be responsible for Fe concentration and nodule formation. Bacteria are a known constituent of Fe–Mn reduction and oxidation processes in soils, and researchers have looked for bacterial processes of Fe–Mn concentration and nodule formation. Babanin et al. (2000) proposed a bacterial source for the magnetic fraction of soil nodules. Counts of Fe-reducing bacteria in nodules and in nodule-containing soils were compared (Babanin et al., 2000). They concluded that reduction of Fe^{3+} occurred at microloci on bacterial cell surfaces because the measured redox potentials in bulk soils were not low enough for Fe reduction. Chan et al. (2004) illustrated how bacterial biofilms became templates for Fe-oxide crystallization. These studies point to bacterial participation in Fe–Mn soil nodule formation but also show that bacterial oxidation is not likely to be the only process involved. A study by He et al. (2008) found the concentration of culturable bacteria within the soil was 10^3 times greater than within the Fe nodules. In that study, either the bacteria were not involved in nodule formation or the bacteria in the nodule could not be cultured by standard methods. We have not investigated the bacterial portion of the Santa Cruz nodules other than to note the presence of some bacterial cells in SEM images.

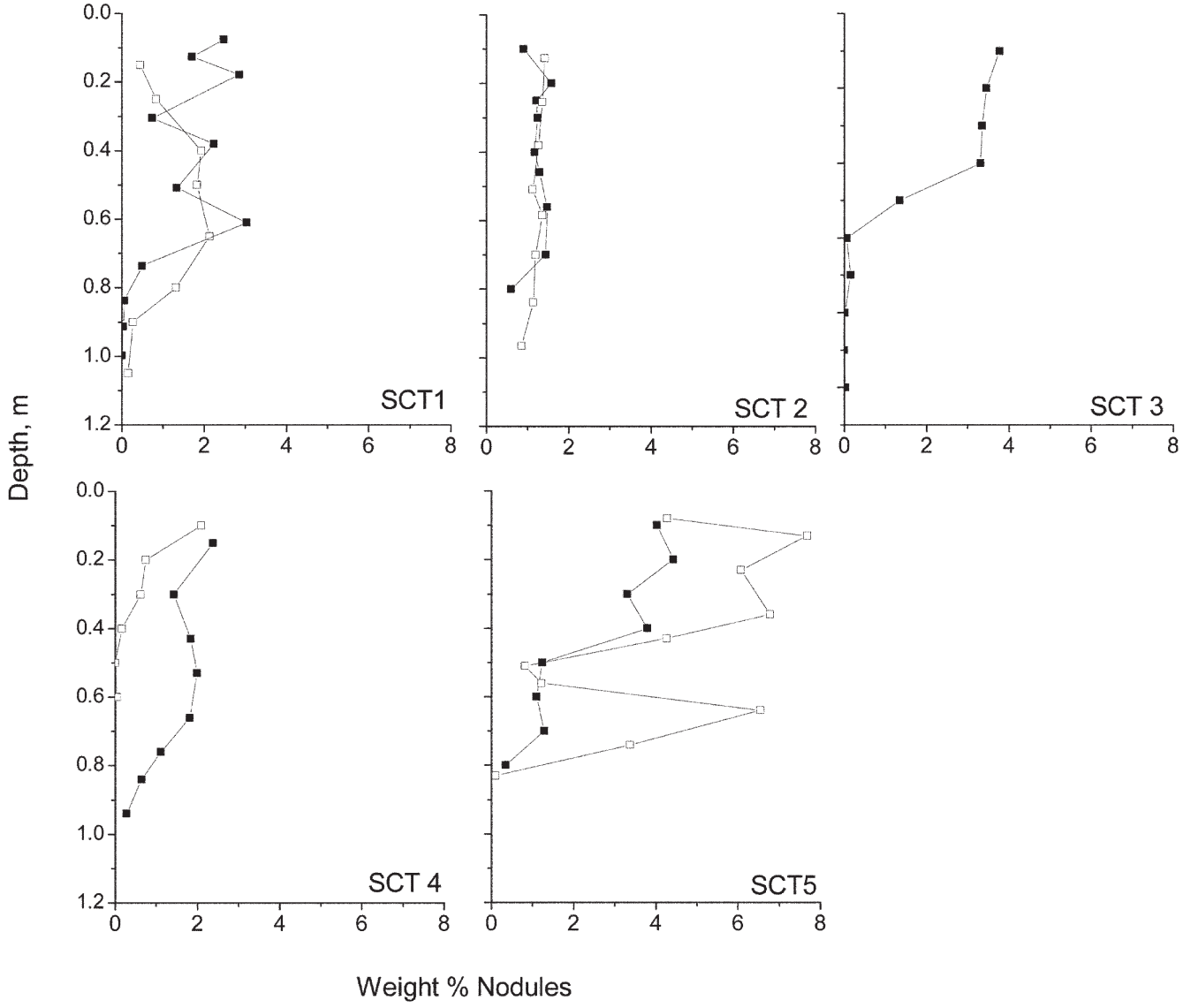

Fig. 8. Nodule abundance and heterogeneity. The SCT4i data from the anthropogenically impacted site is shown with open squares.

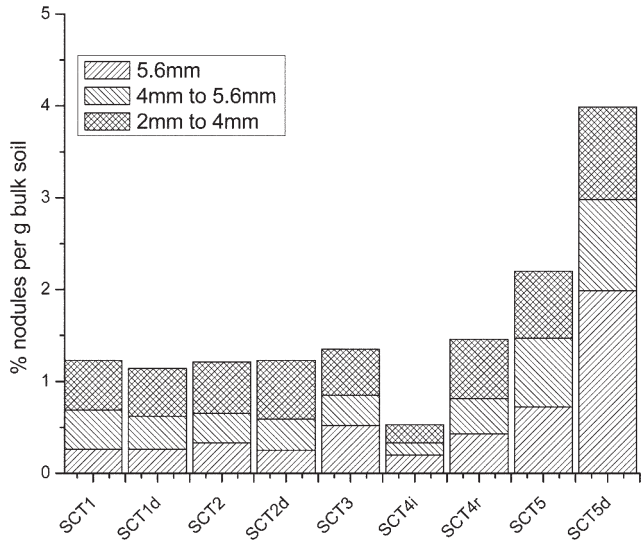

Fig. 9. Nodule abundance by size fraction.

It is the fungal structures that dominate in the Santa Cruz terrace nodules. Fungal features have been reported in other Fe–Mn soil nodules (Zauyah and Bisdom, 1983; Abreu, 1990; Arocena and Pawluk, 1991; Zhang and Karathanasis, 1997; Kovda et al., 1998; Palumbo et al., 2001). In addition, fungal precipitation of metal oxides has been previously reported. Fungal oxidation of Mn has been reported by Golden et al. (1992) and Thompson et al. (2005). Fungi have also been found to oxidize Fe (Feldmann et al., 1997). In addition, it is well established that soil fungi have developed a strategy for Fe mobilization and uptake using exudates (Robin et al., 2008; Winkelmann, 2007). Several studies have reported or shown SEM images with areas of high Fe concentration in soil nodules similar to those found in the Santa Cruz soils (Dawson et al., 1985; Kovda et al., 1998; Cornu et al., 2005). Arocena and Pawluk (1991), after finding fungal hyphae in nodules in Alberta, Canada, measured the ergosterol content of the nodules and the soil matrix. Ergosterol has been used to estimate fungal growth. In their study, the nodules had almost double the ergosterol as the soil matrix.

Collectively, the presence of fungi in nodules from many sites implicates fungi as a possible participant in the soil nodule-forming process. The literature shows that Fe-rich soil nodules are not all formed by the same processes. In some places Fe oxidation and reduction in saturated soils created soil nodules, in other areas the breakdown of a fragipan or dense B horizon created Fe-rich nodules. Abundant fungi in soil Fe nodules have been noted, but attributing the nodule formation to the fungi has not been previously attempted.

Table 3. Iron oxide content of nodules from Santa Cruz terraces (SCT) by inductively couple plasma mass spectrometry and C and N by elemental analyzer.

Element	Nonmagnetic nodules					Magnetic nodules			
	SCT1	SCT2	SCT3	SCT4	SCT5	SCT2	SCT3	SCT4	SCT5
					% (w/w)				
Fe_2O_3	23.3	28.6	25.5	28.4	31.2	37.5	33.5	40.9	42.5
Al_2O_3	7.5	7.8	11.9	10.1	9.9	6.9	7.5	7.0	7.2
MnO	0.235	0.121	0.085	0.031	0.028	0.078	0.046	0.028	0.026
Na_2O	1.176	0.423	0.352	0.195	0.174	0.378	0.339	0.172	0.155
MgO	0.320	0.226	0.283	0.171	0.140	0.259	0.185	0.134	0.106
K_2O	1.018	1.130	1.205	0.907	0.865	1.193	1.078	0.946	0.754
CaO	0.675	0.263	0.237	0.144	0.148	0.248	0.201	0.163	0.147
TiO_2	0.311	0.351	0.564	0.603	0.509	0.435	0.662	0.746	0.616
P_2O_5	0.345	0.321	0.236	0.241	0.237	0.408	0.232	0.280	0.308
SiO_2†	65.1	60.8	59.7	59.2	56.8	52.6	56.3	49.6	48.2
C	0.57	0.99	0.87	0.86	0.72	0.81	0.69	0.84	0.62
N	0.038	0.050	0.040	0.041	0.027	0.500	0.032	0.038	0.022

† SiO_2 by difference.

Nodule Formation in the Santa Cruz Terrace Soils

The Fe nodules in the Santa Cruz chronosequence have areas of high Fe concentration that are associated with oval vesicular structures (Fig. 7). After consulting microbiologists and searching widely for analogous structures in the literature, the similarity of microcolonial fungi (MCF) to the oval vesicular structures found in the nodules was considered an important clue. Microcolonial fungi have been found in some desert varnish ecosystems (Staley et al., 1982; Taylor-George et al., 1983; Perry et al., 2007). The oval vesicular features might have been produced by previously unidentified soil-inhabiting microfungi. As yet no biologic verification of this hypothesis has occurred. If these are fungal structures, then the question arises, "Are the fungi actively precipitating the Fe, or are the fungi being replaced by Fe?" Desert varnish MCF do not have as high an Fe content as the vesicular areas of this study; however, the high-magnification image of a vesicle wall (Fig. 4D, inset) shows Fe oxides as microcrystallites suspended in a matrix. Energy dispersive spectroscopy analyses of the vesicle wall confirmed the presence of Fe and C. This implies that the microcrystalline Fe oxides were bound by an organic matrix and were actively precipitated by the microorganism. In addition, fungal hyphae occupying tunnels within the primary mineral grains also contained Fe. It is known that fungi can accumulate metals intracellularly (Gadd, 1993). Perhaps the nodules of these soils represent a previously unknown type of fungal Fe accumulation.

Further support of a biologic origin comes from the images of small nodules found in a bulk-soil, grain-mount thin section from SCT1 (Fig. 12). These small nodules provide a view of nodule genesis. The incipient nodules have irregular edges. On the outer edge of the nodule, the areas of Fe concentration have begun to cement sand grains. In the center of the nodule, mineral grains are fully embedded in Fe. Of the most compelling interest is the filamentous nature of the Fe-rich area on the outer edge of the nodule (Fig. 12B), which connects bulbous Fe structures. Similar structures were found in a SCT1 nodule split open for SEM examination (Fig. 13). The ball (vesicular) structures are enmeshed in a mycelial network. The mycelium and the ball structures are Fe rich.

Of all the strange structures encountered in the nodules of this study, the hardest to account for have been the structures like those shown in Fig. 14. These images are from a nodule of SCT1,

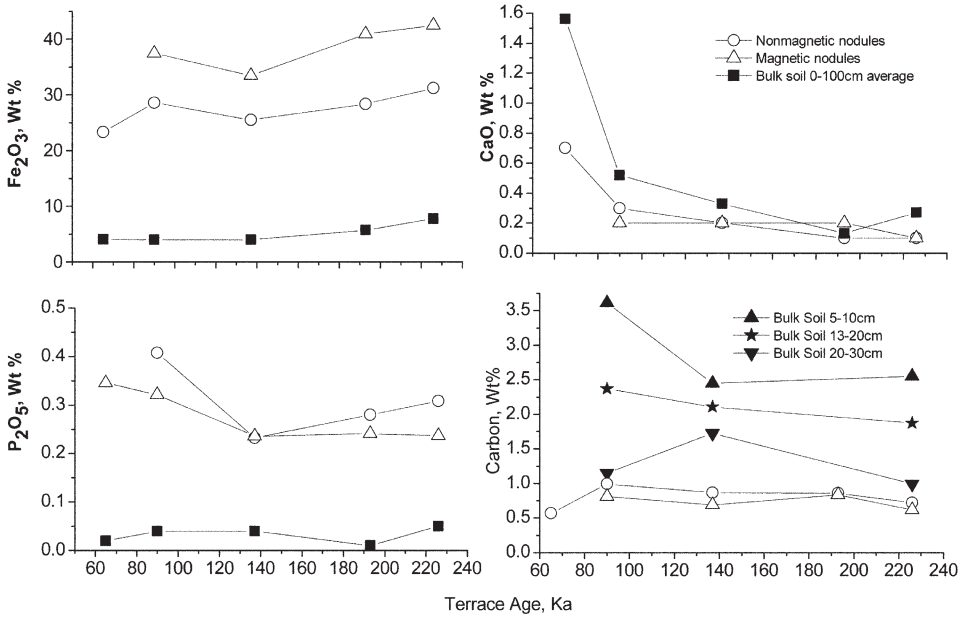

Fig. 10. Iron nodule and bulk soil concentrations of Fe_2O_3, CaO, P_2O_5, and C across the chronosequence. Bulk soil C analyses are from C. Maseillo of Rice University (personal communication, 2009).

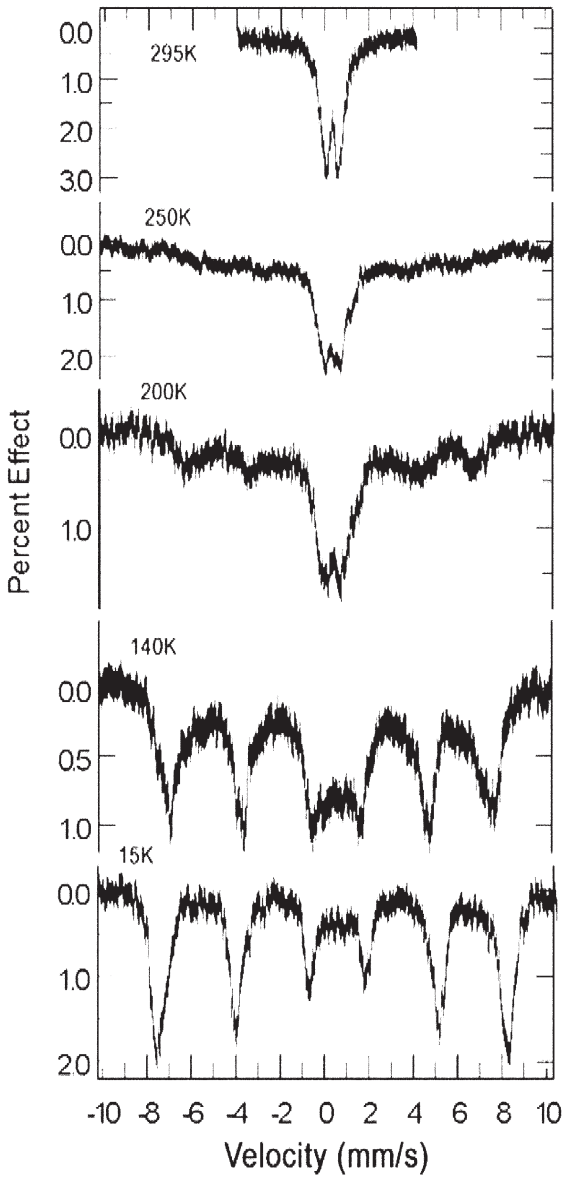

Fig. 11. Mössbauer spectra of SCT1 nonmagnetic nodules. The spectra are plots of the transmission of γ-rays vs. the velocity of the γ-ray source (^{57}Co).

therefore they probably are young, primary structures that have not "matured" or been reworked with time. The boxwork structures (Fig. 14) are both made of Fe oxides that formed around and between the mineral grains. A mineral remnant (starred) can be seen enclosed within the lower structure. There are associated hyphae and perhaps bacterial cells that have dried and flattened on the surfaces of these structures. That fungi can create such features may seem unlikely; however, it is known that fungal aggregates can become glued together as "conglutinate cells" and do form complex biological systems (Read, 2006).

From the morphologic data, we hypothesize that Fe nodules in these soils are the result of fungal growth. In addition, there is evidence of a strategy to sequester mineral nutrients, perhaps utilizing the absorptive properties of Fe oxides. It is well established that fungi in symbiotic relationship with plants will consume and share mineral nutrients (Jongmans et al., 1997; Sterflinger, 2000; van Breemen et al., 2000; Burford et al., 2003; Hoffland et al., 2004; Smits, 2005; Leake et al., 2008; van Scholl et al., 2008). An additional support for this hypothesis is the common occurrence of fungal tunneling in primary minerals in the nodules. The fungal trapping of nutrients with Fe oxides might be quite common and only leave hard nodules under certain conditions, such as in soils with annual wetting–drying cycles, such as a Mediterranean climate.

There is an indication in our data that the fungi responsible for nodule formation are not able to function in an aquic soil moisture regime. Large, hard nodules do not occur in soils near our sites that have an aquic moisture regime. In addition, older soils of the chronosequence have seasonally perched water above an argillic horizon. In these soils, the nodule abundance dropped to near zero below the 60-cm soil depth (Fig. 8). In the better drained soils of SCT1, SCT2, and SCT4r, the nodules extended down to the 100-cm soil depth. As the argillic horizon developed and became an aquitard with perched water during the winter, the nodules seemed to no longer form and any existing nodules may have dissolved. Another compelling observation, from the literature, is that nodules are concentrated in "nests." Both Robbins et al. (1992) and Blagoveschensky and Samsonova (1999) used this term in describing nodule distribution in soils. This suggests that certain areas of the soil landscape are more favorable for nodule formation than others. Clearly more work is needed.

The rounded nodule shape may occur through the combination of several processes. We observed (by SEM) collapsed vesicular structures in several nodules; it seems that the nodule internal morphology degrades with time, older vesicular areas collapsing into a compacted form. The constant bioturbation of soil materials by pocket gophers, worms, etc., disrupts and disperses the Fe nodules. In addition, continual remobilization of Fe on the outer margin through abiotic and biotic processes will, with time, smooth the nodule surface. A slight increase in hematite content in the nodules with time was seen by XRD, indicative of the internal Fe restructuring as the organic fungal structures degraded.

In summary, the data collected by this study led us to the conclusion that the Fe nodules were biologically precipitated by soil fungi or a community of fungi and bacteria.

Formation of Magnetic Nodules

Magnetic nodule abundance increased with soil age. The SCT1 terrace contained only three or four magnetic nodules in the bulk soil samples of the full 1-m profile. In SCT5, magnetic nodules were 33% of the total nodules at the 0.15-m depth. The concentration of magnetic nodules was spatially heterogeneous. Morphologically, the magnetic nodules tended to be smaller. The internal micromorphology of the magnetic nodules was similar to that of the nonmagnetic nodules, indicating that the initial processes of formation were probably similar. The current evidence suggests that a nonmagnetic nodule evolves to a magnetic nodule. We inferred that the occurrence of fire has facilitated a phase change from goethite to maghemite. Magnetic nodules

have been reported at other locations (Kovda et al., 1998; Babanin et al., 2000, 2007). The transformation of goethite to maghemite with heat has been documented by Ketterings et al. (2000). Hanesch et al. (2006) have shown that goethite will convert to maghemite if organic C is present at a temperature of 400 to 450°C. We know that fire plays a role in ecosystem dynamics on the terraces and have measured temperatures of 400°C in a controlled burn through the SCT2 site. In addition, California State Park personnel have observed that duff and shallow roots can smolder for months after a fire, which would bake the surrounding soil (Tim Hyland, personal communication, 2007). There is also an increase in maghemite with time in the <2-mm fraction of the Santa Cruz terrace soils (Aniku and Singer, 1990; Singer et al., 1992), which probably is fire induced. The magnetic nodules are an indicator of fire as a regular ecological occurrence across the terraces.

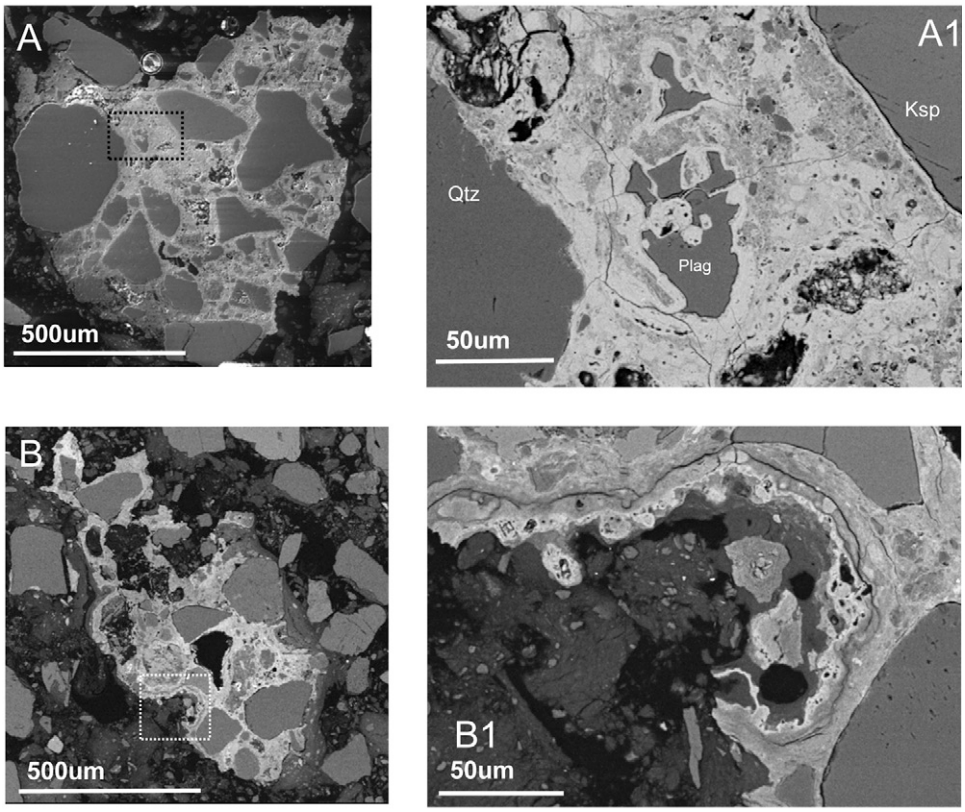

Fig. 12. Scanning electron microscope backscatter images of thin sections of small nodules from SCT1 showing nodule formation. Bright areas are higher in Fe as determined by energy dispersive spectroscopy. Areas indicated in A and B are enlarged in A1 and B1; A1 illustrates the dense, Fe-rich area around a plagioclase feldspar. Note the filamentous nature of the Fe-rich area in B1. Quartz in indicated by Qtz, K-feldspar by Ksp, and plagioclase feldspar by Plag.

CONCLUSIONS

The Fe nodules formed in the soils of the Santa Cruz chronosequence increased in abundance with terrace age and did not occur in the underlying regolith. Nodules were typically microcrystalline goethite with a subset of maghemite nodules (magnetic). There was a slight transformation to hematite with time. Scanning electron microscopy revealed Fe-oxide-containing fungal hyphae throughout the nodules, including vesicular organic structures with embedded fine-grained Fe oxides. The microcrystalline nature of the Fe oxides was substantiated by Mössbauer spectroscopy.

Our morphologic observations led to the hypothesis that the nodules in the Santa Cruz terrace soils were biologically precipitated by fungi or a consortium of fungi and bacteria, perhaps as a strategy to sequester primary mineral grains for nutrient extraction. The fungal structures were probably fixed by seasonal wetting and drying cycles. The organic structures were compacted and the Fe-oxide mineralogy modified by the degradation of fungal C with time. If the nodules were indeed precipitated through fungal processes, there may be tremendous implications for bioremediation of trace metals with a strong affinity for Fe oxides. If we can cultivate Fe-precipitating fungi, a living barrier for contaminant remediation may be possible.

ACKNOWLEDGMENTS

We thank USGS colleagues Jayne Belnap and Tom Huntington for helpful early reviews of the manuscript. We thank the rangers and staff at Wilder State Park, specifically Tim Hyland for his help in the field. We thank Stephanie Mills of Laguna Ranch for providing access for all

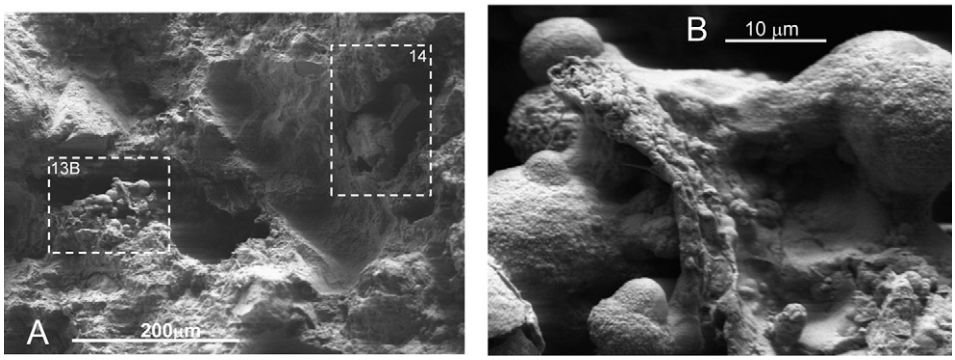

Fig. 13. Scanning electron microscope images from a nodule of SCT1 (low voltage): (A) the "big picture"—note the mineral grains embedded in Fe oxides and hollows where mineral grains have been plucked out by sample preparation—an agglomeration of vesicles enmeshed in mycelia is visible in the boxed area; (B) an enlargement of the right-hand boxed area in A. When analyzed by energy dispersive spectroscopy, all these features contain Fe and C. The boxed area to the left is enlarged in Fig. 14.

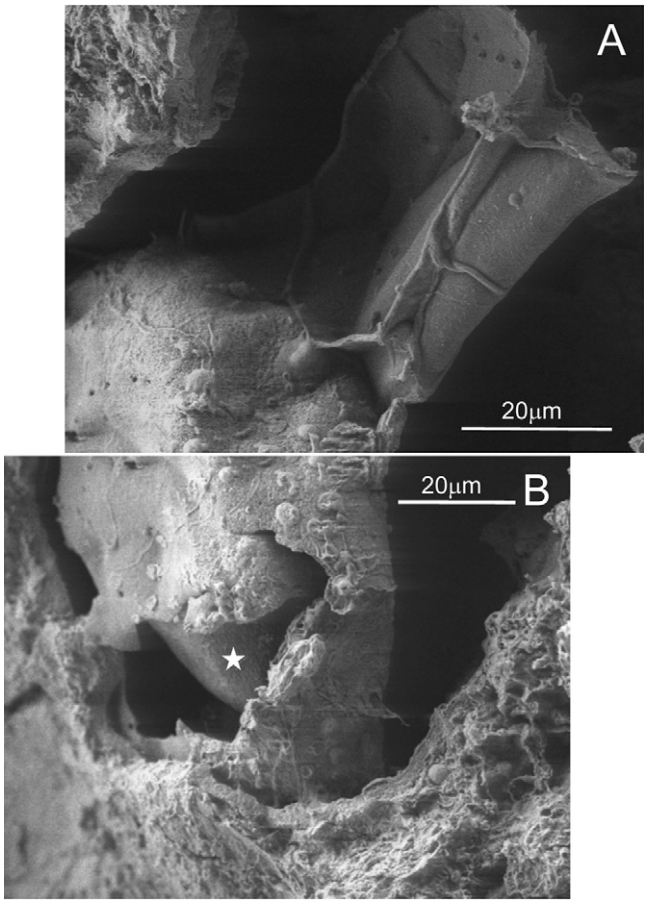

Fig. 14. Scanning electron microscope images (low voltage) of the area indicated in Fig. 13A. We interpreted these boxwork structures as mineral encasements that were disrupted when the nodule was broken. The star in B indicates the enclosed primary mineral. Energy dispersive spectroscopy analysis of this mineral was not possible due to the angle and the deep hole in which the mineral was located. The "outside" of these structures are coated with hyphae and the round objects that may be flattened bacterial cells. Note the regularly spaced holes in the Fe-oxide coating from the outside (B) and inside (A).

the years of the study. We would like to acknowledge the following for helpful discussions and for assistance in the field: Dave Stonestrom, Jennifer Harden, Jennie Munster, and Carrie Maseillo. We thank Jim Hein for the use of the x-ray diffraction laboratory, Robert Oscarson for his assistance in the SEM and microprobe labs, and Renata Mendieta for C content analyses.

REFERENCES

Abreu, M.M. 1990. Ferruginous pisolites from south of Portugal: Paleoenvironmental Quaternary relics. Sci. Geol. Bull. 43:95–102.

Aniku, J.R.F., and M.J. Singer. 1990. Pedogenic iron oxide trends in a marine terrace chronosequence. Soil Sci. Soc. Am. J. 54:147–152.

Arocena, J.M., and S. Pawluk. 1991. The nature and origin of nodules in podzolic soils from Alberta. Can. J. Soil Sci. 71:411–426.

Babanin, V.F., D.E. Ivanov, D.E. Pukhov, and A.M. Shipilin. 2000. Magnetic properties of concretions in surface-gleyed podzolic soils. Eurasian Soil Sci. 33:1072–1079.

Babanin, V.F., V.I. Nikolaev, D.E. Pukhov, A.M. Shipilin, and O.A. Shirmina. 2007. Diagnostics of manganese–iron nodules in soddy-podzolic soils at different degrees of gleyzation from their magnetic properties. Eurasian Soil Sci. 40:247–255.

Betancur, J.D., C.A. Barrero, J.M. Greneche, and G.F. Goya. 2004. The effect of water content on the magnetic and structural properties of goethite. J. Alloys Compounds 369:247–251.

Blagoveschensky, Y.N., and V.P. Samsonova. 1999. Fractal and the statistical analysis of spatial distributions of Fe–Mn concretions in soddy-podsolic soils. Geoderma 88:265–282.

Bowman, R.H., and D.C. Estrada. 1980. Soil survey of Santa Cruz County, California. U.S. Gov. Print. Office, Washington, DC.

Bradley, W.C. 1957. Origin of marine-terrace deposits in the Santa Cruz area, California. Geol. Soc. Am. Bull. 68:421–444.

Bradley, W.C., and G.B. Griggs. 1976. Form, genesis, and deformation of central California wave-cut platforms. Geol. Soc. Am. Bull. 87:433–449.

Brown, I.C., and J. Thorp. 1942. Morphology and composition of some soils of the Miami family and Miami catena. USDA Tech. Bull. 834. U.S. Gov. Print. Office, Washington, DC.

Burford, E.P., M. Fomina, and G.M. Gadd. 2003. Fungal involvement in bioweathering and biotransformation of rocks and minerals. Mineral. Mag. 67:1127–1155.

Chan, C.S., G. De Stasio, S.A. Welch, M. Girasole, B.H. Frazer, M.V. Nesterova, S. Fakra, and J.F. Banfield. 2004. Microbial polysaccharides template assembly of nanocrystal fibers. Science 303:1656–1658.

Cornu, S., V. Deschatrettes, S. Salvador-Blanes, B. Clozel, M. Hardy, S. Branchut, and L. Le Forestier. 2005. Trace element accumulation in Mn–Fe-oxide nodules of a planosolic horizon. Geoderma 125:11–24.

da Costa, G.M., E. De Grave, L.H. Bowen, P.M.A. de Bakker, and R.E. Vandenberghe. 1995. Variable-temperature Mössbauer spectroscopy of nano-sized maghemite and Al-substituted maghemites. Clays Clay Miner. 43:562–568.

Dawson, B.S.W., J.E. Fergusson, A.S. Campbell, and E.J.B. Cutler. 1985. Distribution of elements in some Fe–Mn nodules and an iron-pan in some gley soils of New Zealand. Geoderma 35:127–143.

Emery, K.O. 1950. Ironstone concretions and beach ridges of San Diego County, California. Calif. J. Mines Geol. 46:213–221.

Feldmann, M., J. Neher, W. Jung, and F. Graf. 1997. Fungal quartz weathering and iron crystallite formation in an alpine environment, Piz Alv, Switzerland. Eclogae Geol. Helv. 90:541–556.

Gadd, G.D. 1993. Interaction of fungi with toxic metals. New Phytol. 124:25–60.

Gaiffe, M., and B. Kubler. 1992. Relationships between mineral composition and relative ages of iron nodules in Jurassian soil sequences. Geoderma 52:343–350.

Golden, D.C., D.A. Zuberer, and J.B. Dixon. 1992. Manganese oxides produced by fungal oxidation of manganese from siderite and rhodochrosite. p. 161–168. *In* H.C.W. Skinner and R.W. Fitzpatrick (ed.) Biomineralization processes of iron and manganese: Modern and ancient environments. Catena Suppl. 21. Catena Verlag, Cremlingen, Germany.

Hanesch, M., H. Stanjek, and N. Petersen. 2006. Thermomagnetic measurements of soil iron minerals: The role of organic carbon. Geophys. J. Int. 165:53–61.

He, J., L. Zhang, S. Jin, Y. Zhu, and F. Liu. 2008. Bacterial communities inside and surrounding soil iron–manganese nodules. Geomicrobiol. J. 25:14–24.

Hoffland, E., T.W. Kuyper, H. Wallander, C. Plassard, A.A. Gorbushina, K. Haselwanter, et al. 2004. The role of fungi in weathering. Front. Ecol. Environ. 2:258–264.

Johnson, D.L. 1972. Landscape evolution on San Miguel Island, California. Ph.D. diss. Dep. of Geography, Univ. of Kansas, Lawrence.

Johnson, D.L. 1988. Age and origin of iron and manganese concretions in soils. p. 281. *In* Abstr., Congr. of the Int. Geograph. Union, 26th, Sydney, Australia. 21–26 Aug. 1988. Univ. of Sydney, Sydney, NSW, Australia.

Jongmans, A.G., N. van Breeman, U. Lundström, P.A.W. van Hees, R.D. Finlay, M. Srinivason, T. Unestam, R. Giesler, P.A. Melkerud, and M. Olsson. 1997. Rock-eating fungi. Nature 389:682–683.

Kemp, R.A., P.A. McDaniel, and A.J. Busacca. 1998. Genesis and relation of macromorphology and micromorphology to contemporary hydrological conditions of a welded Argixeroll from the Palouse in Idaho. Geoderma 83:309–329.

Ketterings, Q.M., J.M. Bigham, and V. Laperche. 2000. Changes in soil mineralogy and texture caused by slash-and-burn fires in Sumatra, Indonesia. Soil Sci. Soc. Am. J. 64:1108–1117.

Kovda, I.V., E.G. Morgun, A.-M. Jaunet, and D. Tessier. 1998. An experience in the submicroscopic study of iron neoformations from Vertisols of the central Ciscaucasian region. Eurasian Soil Sci. 31:594–604.

Latrille, C., F. Elass, F. van Oort, and L. Denaix. 2001. Physical speciation of trace metals in Fe–Mn concretions from a rendzic lithosol developed on Sinemurian limestones (France). Geoderma 100:127–146.

Leake, J.R., A.L. Duran, K.E. Hardy, I. Johnson, D.J. Beerling, S.A. Banwart, and

M.M. Smits. 2008. Biological weathering in the soil: The role of symbiotic root-associated fungi biosensing minerals and directing photosynthate-energy into grain-scale mineral weathering. Mineral. Mag. 72:85–89.
Lindbo, D.L., F.E. Rhoton, W.H. Hudnall, N.E. Smeck, J.M. Bigham, and D.D. Tyler. 2000. Fragipan degradation and nodule formation in Glossic Fragiudalfs of the Lower Mississippi River Valley. Soil Sci. Soc. Am. J. 64:1713–1722.
Liu, F., C. Colombo, P. Adamo, J.Z. He, and A. Violante. 2002. Trace elements in manganese–iron nodules from a Chinese Alfisol. Soil Sci. Soc. Am. J. 66:661–670.
Maher, K., C.I. Steefel, A.F. White, and D.A. Stonestrom. 2009. The role of reaction affinity and secondary minerals in regulating chemical weathering rates at the Santa Cruz soil chronosequence, California. Geochim. Cosmochim. Acta 73:2804–2831.
Manceau, A., N. Tamura, R.S. Celestre, A.A. Macdowell, N. Geoffroy, G. Sposito, and H.A. Padmore. 2003. Molecular-scale speciation of Zn and Ni in soil ferromanganese nodules from loess soils of the Mississippi Basin. Environ. Sci. Technol. 37:75–80.
Manies, K., J.W. Harden, and H. Veldhuis. 2006. Soil data from a moderately well and somewhat poorly drained fire chronosequence near Thompson, Manitoba, Canada. Open-File Rep. 2006-1291. USGS, Reston, VA.
Mitra, S. 1992. Applied Mössbauer spectroscopy: Theory and practice for geochemists and archaeologists. Pergamon Press, Oxford, UK.
Moody, L.E., and R.C. Graham. 1995. Geomorphic and pedogenic evolution in coastal sediments, central California. Geoderma 67:181–201.
Muhs, D.R. 1982. A soil chronosequence on Quaternary marine terraces, San Clemente Island, California. Geoderma 28:257–283.
Munster, J., and J.W. Harden. 2002. Physical data of soil profiles formed on Late Quaternary marine terraces near Santa Cruz, California. Open-File Rep. 02-316. USGS, Reston, VA.
Palumbo, B., A. Bellanca, R. Neri, and M.J. Roe. 2001. Trace metal partitioning in Fe–Mn nodules from Sicilian soils, Italy. Chem. Geol. 173:257–269.
Perg, L.A., R.S. Anderson, and R.C. Finkle. 2001. Use of a new ^{10}Be and ^{26}Al inventory method to date marine terraces, Santa Cruz, California, USA. Geology 29:879–882.
Perry, R.S., N. Mcloughlin, B.Y. Lynne, M.A. Sephton, J.D. Oliver, C.C. Perry, K. Campbell, M.H. Engel, J.D. Farmer, M.D. Brasier, and J.T. Staley. 2007. Defining biominerals and organominerals: Direct and indirect indicators of life. Sediment. Geol. 201:157–179.
Phillippe, W.R., R.L. Blevins, R.I. Barnhisel, and H.H. Bailey. 1971. Distribution of concretions from selected soils of the Inner Bluegrass region of Kentucky. Soil Sci. Soc. Am. J. 36:171–173.
Pinney, C., J.R.F. Aniku, R. Burke, J.W. Harden, M.J. Singer, and J. Munster. 2002. Soil chemistry and mineralogy of the Santa Cruz coastal marine terraces. Open-File Rep. 2002-277. USGS, Reston, VA.
Read, N.D. 2006. Environmental sensing and the filamentous fungal lifestyle. p. 38–57. *In* G.M. Gadd (ed.) Fungi in the environment. Cambridge Univ. Press, Cambridge, UK.
Robbins, E.I., J.P. D'Agostiono, J. Ostwald, D.S. Fanning, V. Carter, and R.L. Van Hoven. 1992. Manganese nodules and microbial oxidation of manganese in the Huntley Meadows wetland, Virginia, USA. Catena Suppl. 21:179–202.
Robin, A., G. Vansuyt, P. Hinsinger, J.M. Meyer, J.F. Briat, and P. Lemanceau. 2008. Iron dynamics in the rhizosphere: Consequences for plant health and nutrition. Adv. Agron. 99:183–225.
Schwertmann, U., and D.S. Fanning. 1976. Iron–manganese concretions in hydrosequences of soils in loess in Bavaria. Soil Sci. Soc. Am. J. 40:731–738.
Singer, M.J., P. Fine, K.L. Verosub, and O.A. Chadwick. 1992. Time dependence of magnetic susceptibility of soil chronosequences on the California coast. Quat. Res. 37:323–332.
Singh, B., and R.J. Gilkes. 1996. Nature and properties of iron rich glaebules and mottles from some southwest Australian soils. Geoderma 71:95–120.
Smits, M.M. 2005. Contribution of fungal tunneling to total feldspar weathering. Geoderma 125:59–69.
Staley, J.T., F. Palmer, and J.B. Adams. 1982. Microcolonial fungi: Common inhabitants on desert rocks? Science 215:1093–1094.
Sterflinger, K. 2000. Fungi as geologic agents. Geomicrobiol. J. 17:97–124.
Stiles, C., C. Mora, and S.G. Driese. 2001. Pedogenic iron–manganese nodules in Vertisols: A new proxy for paleoprecipitation? Geology 29:943–946.
Taylor-George, S., F. Palmer, J.T. Staley, D.J. Borns, B. Curtiss, and J.B. Adams. 1983. Fungi and bacteria involved in desert varnish formation. Microb. Ecol. 9:227–245.
Thompson, I.A., D.M. Huber, C.A. Guest, and D.G. Schulze. 2005. Fungal manganese oxidation in a reduced soil. Environ. Microbiol. 7:1480–1487.
Tiessen, H., M.K. Abekoe, I.H. Salcedo, and E. Owusu-Bennoah. 1993. Reversibility of phosphorus sorption by ferruginous nodules. Plant Soil 153:113–124.
Trenhaile, A.S. 2005. Modelling the effect of waves, weathering and beach development on shore platform development. Earth Surf. Processes Landforms 30:613–634.
Uzochukwu, G.A., and J.B. Dixon. 1986. Manganese oxide minerals in nodules of two soils of Texas and Alabama. Soil Sci. Soc. Am. J. 50:1358–1363.
van Breemen, N., U. Lundstrom, A.G. Jongmans, R. Gieler, and M. Olsson. 2000. Mycorrhizal weathering: A true case of mineral plant nutrition? Biogeochemistry 49:53–67.
van Scholl, L., T.W. Kuyper, M.M. Smits, R. Landeweert, E. Hoffland, and N. van Breeman. 2008. Rock-eating mycorrhizas: Their role in plant nutrition and biogeochemical cycles. Plant Soil 303:35–47.
Weber, G.E., and A.O. Allwardt. 2001. The geology from Santa Cruz to Point Año Nuevo: The San Gregorio fault zone and Pleistocene marine terraces. p. 1–32. *In* P.W. Stoffer and L.C. Gordon (ed.) Geology and natural history of the San Francisco Bay area. USGS Bull. 2188. USGS, Menlo Park, CA.
White, A.F., M.S. Schulz, D.A. Stonestrom, D.V. Vivit, J. Fitzpatrick, T.D. Bullen, K. Maher, and A.E. Blum. 2009. Chemical weathering of a marine terrace chronosequence, Santa Cruz, California: II. Solute gradients and linear approximations of contemporary and long-term weathering rates. Geochim. Cosmochim. Acta 73:2769–2803.
White, A.F., M.S. Schulz, D.V. Vivit, A.E. Blum, D.A. Stonestrom, and S.P. Anderson. 2008. Chemical weathering of a marine terrace chronosequence, Santa Cruz, California: I. Interpreting rates and controls based on soil concentration–depth profiles. Geochim. Cosmochim. Acta 72:36–68.
Winkelmann, G. 2007. Ecology of siderophores with special reference to the fungi. BioMetals 20:379–392.
Zauyah, S., and E.B.A. Bisdom. 1983. SEM-EDXRA investigation of tubular features and iron nodules in lateritic soils from Malaysia. Geoderma 30:219–232.
Zhang, M., and A.D. Karathanasis. 1997. Characterization of iron–manganese concretions in Kentucky Alfisols with perched water tables. Clays Clay Miner. 45:428–439.